Preparation and Characterization of New Magnetic Montmorillonite Clay Mineral by Intercalation of Iron Oxides in West Iraqi Layered Bentonite

Mohammed H. Abdul Latif*,   Furat Latif Yahya

Department of Chemistry, Ibn Al Haitham College of Education, University of Baghdad , Adhamiya, Al- Dilal Square, Baghdad, Iraq.

Abstract

A new magnetic montmorillonite hybrid materials of iron (Fe II, Fe III) with Iraqi (Traifawi) montmorillonite were synthesized by mixing 15 g. of H – form initiated montmorillonite with 100 ml saturated aqueous solutions of different percent ratios of ferric and ferrous chlorides ($FeCl_3$ & $FeCl_2$) with continuous agitation at 60ºC, and the mixture is allowed to react for 24 h. to ensure maximum interlayer (Fe^{+3} & Fe^{+2}) cations intercalation. The resulting Fe – intercalated montmorillonite solids were separated by centrifugation, washed several times with deionized water to free Hydrochloric acid (HCl), dried at 100 ºC for 24 h. (Fe II, Fe III) –montmorillonite was characterized by Magnetic susceptibility measurement, X-ray diffraction (XRD), FT-IR spectroscopy, and scanning electron microscopy (SEM). The intercalated bentonite samples show high Magnetic susceptibilities due to increment or decrement of Magnetite and Hematite content in these clay samples. All the XRD patterns of iron (Fe II, Fe III) montmorillonite nanocomposites shows a red shift in the position of Montmorillonite mineral main peak due to the emergence of new magnetic clay mineral by intercalation of (Fe II, Fe III) in montmorillonite. Also the clay reflections, present some additional peaks that obviously originate from iron oxides (Hematite Fe_2O_3), and (Magnetite Fe_3O_4). FT-IR patterns of (Fe II, Fe III) – montmorillonite samples noticed the appearance of new peaks belongs to (Hematite) Fe_2O_3 stretching vibration, Fe-O stretching vibration, and (Magnetite Fe_3O_4) stretching vibration. SEM images of (Fe II, Fe III) – montmorillonite samples showed a change in the nature of the Montmorillonite clay surface.

Keywords: Intercalation, West Iraqi, Magnetic Montmorillonite, Layered Bentonite.

1.   Introduction

Magnetic nanoparticles have been prepared by various methods such as arc discharge, mechanical grinding, laser ablation, micro emulsion, and high temperature decomposition of organic precursors [1]. Magnetic particles can be used to adsorb contaminants from aqueous or gaseous effluents and after the adsorption is carried out, the adsorbent can be separated from the medium by a simple magnetic process. Some examples of this technology are the use of magnetite particles to accelerate the coagulation of sewage [2], In order to protect the magnetic NPs against oxidation; a shell structure is often introduced, such as a silica shell or polymer shell [3]. Several methods have been accordingly developed to minimize the co aggregation of nanoparticles (in which case, leads to decrease the effective surface area of nanoparticles and thus reduce their reaction activities), obtain the soft sediment, and improve their manipulation, such as supporting of magnetic nanoparticles on polymers or inorganic matter, like porous silica [4, 5]. In recent years, considerable attention has been paid to iron oxides, especially on magnetic (Fe_3O_4) nanoparticles (Figure 1) due to their potential applications such as pigment, magnetic resonance imaging, magnetic drug delivery, Ferro fluids, recording material, and data storage media [6, 7].
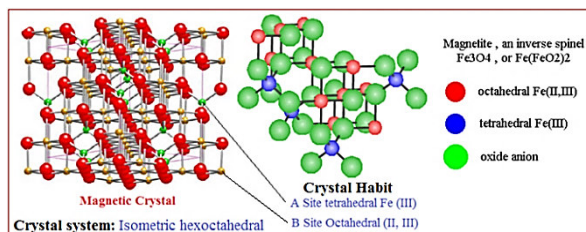

Figure 1: Magnetite crystal lattice system.

Magnetite is an iron catalyst with a central role in the industrial Haber–Bosch process for the production of ammonia [8]. Magnetic nanoparticles and their composites are extremely suitable in water treatment for the coagulation of sewage [9] or for the complete elimination of contaminants from drinking water sources such as heavy metals [10]. Besides these conventionally considered fields, magnetic materials became highlighted in nanoscience, medicine, and biotechnology, serving as high density recording media [11], novel recoverable enzyme or drug carriers [12–14] or tools for the separation and purification of biomolecules and cells in bioprocesses [15, 16]. Clay minerals are the most common inorganic materials on the earth's surface with crystalline alumino silicate structure. They are mostly used in various fields including Nano composites,

building materials, ceramics, paper coatings, pharmaceuticals, adsorbents, ion exchangers, separators, catalysts, and as the supporting materials of magnetic nanoparticles, due to their great abundance, environmental friendly, low cost, and particular properties [17]. Natural clays are low-cost and readily available materials functioning as excellent cation exchangers, which have often been used to adsorb metallic contaminants. The adsorption capacity of clays results from a relatively high surface area and a net negative charge on their structure, which attracts and holds cations such as heavy metals [18]. The layered clays used for these purposes are Kaolin, Montmorillonite, mica, Sericite, Hydrotalcite, Fluoromica, Hectorite, and Saponite, but one of the most commercially interesting clays is Bentonite [Montmorillonite (MMT) $(Na_{0.7} (Al_3.3Mg_{0.7}) Si_8O_{20} (OH)_4. nH_2O)]$, which have the smallest crystals, the largest surface area, and the highest cation exchange capacity (CEC) [19], belonging to a structural family known as the 2:1 phyllosilicates. Its inner layers are composed of an octahedral sheet, which is situated between two tetrahedral sheets (Figure 2), is known as a polymer modifier due to its high specific surface area [20]. Such layers are stacked by weak dipolar or van der Waals forces, leading to the interaction of charge compensating cations into the interlayer space. Therefore, not only adsorption on the external surface but also intercalation into the interlayer space can occur [21].
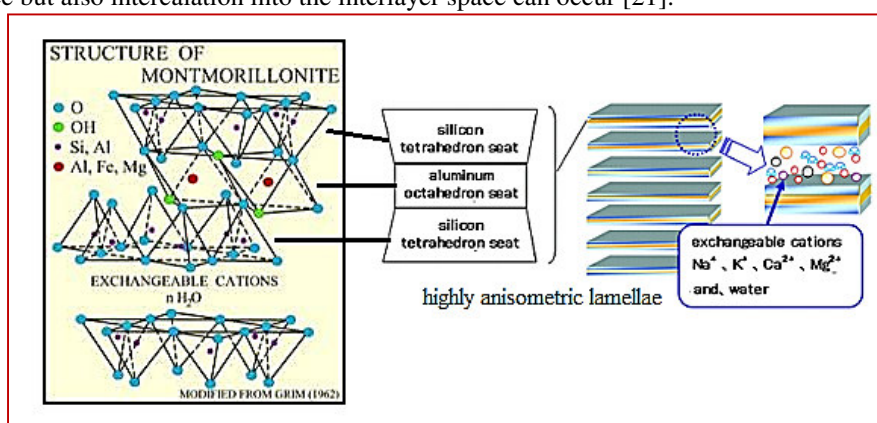

Figure 2; The Structure of montmorillonite clay mineral.

Montmorillonite (MMT clay minerals having highly anisometric lamellae can be readily used as anti-settling agents to slow down the sedimentation and to obtain soft sediment and, moreover, their cation exchange properties make them outstandingly suitable starting materials for the preparation of metal oxide Nano composites. Magnetic iron oxide/montmorillonite hybrid materials have been described in the literature, including both magnetite (Fe_3O_4) and Maghemite $(\gamma-Fe_2O_3)$ [8]. Magnetite and Maghemite are ferromagnetic iron oxides with a very similar structure. Magnetite, Fe_3O_4, also known as lodestone, adopts a cubic spinel structure with the lattice parameter of 8.394 A°. Fe^{3+} cations are arranged in tetrahedral positions, and Fe2+ and the remaining Fe3+ are randomly distributed in the octahedral ones. Maghemite, $\gamma-Fe_2O_3$, also possesses a spinel structure with Fe3+ cations in both tetrahedral and octahedral sites. The unit cell is tetragonal with c/a = 3. It is made by piling up three cubic spinel cells of Fe_3O_4 and removing eight Fe atoms from octahedral sites. Therefore, it is not easy to distinguish between the two oxides or quantify their presence in materials by means of traditional structural techniques such as XRD or TEM [22]. Modification of clays by the intercalation of cationic complexes of metals into the swelled interlayer region followed by calcination allows the preparation of thermally stable microporous solids, named pillared clays (PILCs). Different oxocations containing Al, Zr, Ti, La, Ga, Cr, or Fe have been used by researchers, who stated that the final PILCs indicate a permanent porous network and increased specific surface area, showing a dramatic improvement in catalytic and adsorption properties. PILCs prepared with iron oxocations (Fe-PILC) have recently been used in a variety of processes, including catalytic degradation of dyes, catalytic reduction of compounds, selective oxidation, adsorptive removal of contaminants, and microbial processes [17]. West Iraqi bentonite consists mostly of calcium – montmorillonite. The percent of montmorillonite is between (60 – 65 %) of crude bentonite, (Table 1) show the chemical analysis of west Iraqi montmorillonite. Therefore it is necessary to remove the impurities before the bentonite is ready to use. The surface area for west Iraqi bentonite was estimated using methylene blue (MB) adsorption method and it was (123 m2 /g) [23].

Table 1. Chemical analysis of West Iraqi Bentonite.

Compound	SiO_2	Al_2O_3	Fe_2O_3	CaO	MgO	Na_2O	K_2O	LiO_2	SO_3	L.I.O.	Total
Weight %	55.81	14.91	5.78	5.72	3.5	1.29	0.41	0.67	----	10.86	99.67

In this work, the adsorption features of clays with the magnetic properties of iron oxides have been combined in a composite to produce a magnetic adsorbent. To do that we report a new easy method of preparation of magnetic montmorillonite hybrid depending on the good ion exchange property of Iraqi montmorillonite clay

minerals, by intercalation mechanism of several percent ratios of ferric and ferrous chlorides ($FeCl_3$ & $FeCl_2$) in (H- form) purified initiated west Iraqi montmorillonite clay mineral using batch method.

2. Experimental

West Iraqi Bentonite (Ca – montmorillonite) clay used in the present study obtained from the General Company for Geological Survey and Mining in Baghdad, Iraq. The cation exchange capacity (CEC) of Ca – montmorillonite is 80 meq. /100 g of clay, and the Ca – montmorillonite percent in crude is between (60 – 65 %). The clay sample was sieved to produce particle size of 45μm, dried for 24 h. at 100 ºC in an electric oven, and stored in a desiccator until use. Activated H – form Amberlight orange ion exchanger and ($FeCl_3$ & $FeCl_2$) were purchased from Fluka-BDH Chemicals. Distilled and deionized water with a conductivity value of 1.5×10^{-5} S Cm^{-1} was used. West Iraqi Ca – montmorillonite was benefitted to improve its montmorillonite content and cation exchange capacity (CEC) by attrition – scrubbing at high concentration (15 %) and at high impeller speed (2500 r.p.m.) for 1 h., using Flotation Cell. The resulting solid was separated by centrifugation, washed several times with deionized water and dried at 100 ºC for 24 hour. Magnetic montmorillonite was prepared by converting (Ca – montmorillonite 15% solution) to (H – montmorillonite) using Activated H – form Amberlight orange ion exchange at the molar ratio of 1:1, followed by agitation for 24 h. at 150 r.p.m. and 60 ºC using thermo stated shaker bath (Alba Tch.). Clay suspension was separated from Amberlight orange ion exchange granules using 75μm sieve. The resulting solid was separated by centrifugation, washed several times with deionized water and dried at 100 ºC for 24 h. Eleven 15 g. sample of the resulting H – form initiated montmorillonite was mixed with 100 ml saturated aqueous solutions of different percent ratios of ferric and ferrous chlorides ($FeCl_3$ & $FeCl_2$) with continuous agitation at 60ºC, and the mixture is allowed to react for 24 h. to ensure maximum interlayer (Fe^{+3} & Fe^{+2}) cations intercalation. The resulting Fe – intercalated montmorillonite solids were separated by centrifugation, washed several times with deionized water to free Hydrochloric acid (HCl), dried at 100 ºC for 24 h. Magnetic susceptibility of samples (1 – 13) were measured by Sherwood Scientific's Magnetic susceptibility balances (Table 2). X-ray diffraction (XRD) diffractogram were obtained for samples of higher magnetic susceptibility (1, 2, 3, 4, 5, 9, and 12) on Shimadzu x- ray diffraction P 04 – XRD – 6000 (Figures 3, 4, 5, 6, 7, 8 and 9). Fourier Transform – Infrared (FT-IR) spectra were recorded for samples of higher magnetic susceptibility (1, 2, 3, 4, 5, 9, and 12) on Shimadzu FT-IR Spectrophotometer – 30000:1/ IRAFF (Figures 10, 11, 12, 13, 14, 15, 16, 17, and 18). SEM Micrographs were carried out for samples (2, 3, and 9) on VEGA3 – TESCAN Scanning Electron Microscope (Figure 19).

3- Result and discussion

3.1. Magnetic susceptibility:

It can be seen from (Table 2) that the Magnetic susceptibility of activated clay sample have risen due to the removal of impurities which increases the effect Magnetite and Hematite found in bentonite clay minerals as a result of containment of clay on both types of iron (Fe II, Fe III). Also we see that the intercalated bentonite samples with different saturated solutions percent of ($FeCl_2$, $FeCl_3$) show different Magnetic susceptibilities due to increment or decrement of Magnetite and Hematite content in these clay samples. Samples show highest Magnetic susceptibilities are samples (no. 3, 4, 5, 9, &, 12).
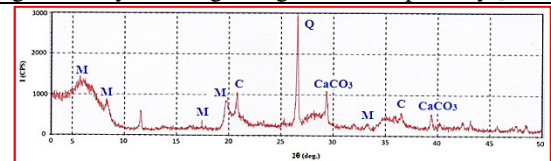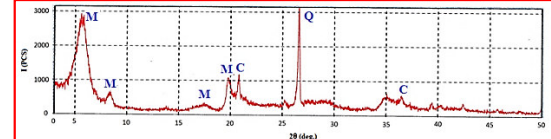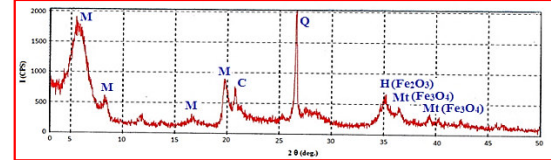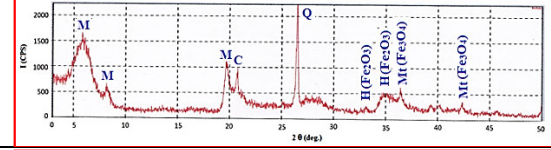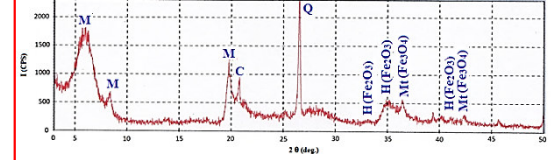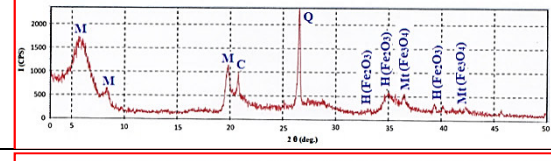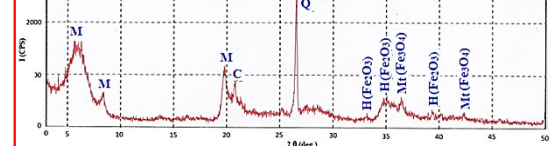
Table 2: Bentonite magnetic susceptibility data   temp. = 20 ºC

No.	Sample Height (mm)	Sample Weight (g)	Sample details	X_g
1	20	0.1350	Crude Bentonite	7.4×10^{-6}
2	20	0.1368	Initiated Bentonite	9.0×10^{-6}
3	20	0.1565	Bentonite 100% $FeCl_2$	9.7×10^{-6}
4	20	0.1380	Bentonite 100% $FeCl_3$	11.5×10^{-6}
5	20	0.1222	Bentonite 50% $FeCl_3$, 50% $FeCl_2$	9.9×10^{-6}
6	20	0.1523	Bentonite 70% $FeCl_3$, 30% $FeCl_2$	8.5×10^{-6}
7	20	0.1620	Bentonite 80% $FeCl_3$, 20% $FeCl_2$	6.6×10^{-6}
8	20	0.1467	Bentonite 60% $FeCl_3$, 40% $FeCl_2$	7.8×10^{-6}
9	20	0.1419	Bentonite 40% $FeCl_3$, 60% $FeCl_2$	9.4×10^{-6}
10	20	0.1661	Bentonite 30% $FeCl_3$, 70% $FeCl_2$	7.8×10^{-6}
11	20	0.1240	Bentonite 20% $FeCl_3$, 80% $FeCl_2$	6.7×10^{-6}
12	20	0.1563	Bentonite 90% $FeCl_3$, 10% $FeCl_2$	9.2×10^{-6}
13	20	0.1684	Bentonite 10% $FeCl_3$, 90% $FeCl_2$	6.4×10^{-6}

3.2. Powder X-ray diffraction Characterization of Montmorillonite clay samples:

Figures (3-9) shows the XRD patterns of crude, activated initiated Montmorillonite clay mineral and those of iron (Fe II, Fe III) montmorillonite nanocomposites. Crude clay reflections (Figure 3), presents some peaks at 2θ = 5.76◦ (I = 1450 CPS, and d spacing = 1.533109 nm), 6.92◦, 8.377◦, 11.5827◦, and 19.78◦, characteristic for

montmorillonite clay mineral, the first one is the main montmorillonite peak. Also there are some additional peaks refer to Cristobalite (C), Quartz (Q), and $CaCO_3$ minerals. Activated initiated Montmorillonite XRD pattern (Figure 4) show that the main montmorillonite peak appear at $2\theta = 5.9579°$ (I = 2910 CPS, and d spacing = 1.48228 nm), and the $CaCO_3$ peaks disappears due to the removal of impurities. This will raise the montmorillonite present in Iraqi bentonite from 65% to more than 90%. All the XRD patterns of iron (Fe II, Fe III) montmorillonite nanocomposites shows a red shift in the position of Montmorillonite mineral main peak due to the emergence of new hybrid magnetic clay mineral by intercalation of (Fe II, Fe III) in montmorillonite. Also the clay reflections, present some additional peaks that obviously originate from iron oxides (Hematite Fe_2O_3), at $(2\theta = 24°, 33°, 34°, 35°, 39°, 41°,$ and $49°)$, and (Magnetite Fe_3O_4), at $(2\theta = 36°, 39°, 42°,$ and $43°)$ these peaks indicates the success of (Fe II, Fe III) intercalation method in montmorillonite clay mineral and reinforce the formation of magnetic clay with high magnetic susceptibility [24 & 25].

Figure 3: Powder X- ray diffraction of crude Iraqi Bentonite.

Figure 4: Powder X- ray diffraction of initiated H-form Iraqi Bentonite.

Figure 5: Powder X- ray diffraction of intercalated Bentonite with 100 % $FeCl_2$

Figure 6: Powder X- ray diffraction of intercalated Bentonite with 100 % $FeCl_3$.

Figure 7: Powder X- ray diffraction of intercalated Bentonite with 40 % $FeCl_3$ + 60 % $FeCl_2$

Figure 8: Powder X- ray diffraction of intercalated Bentonite with 50 % $FeCl_3$ + 50 % $FeCl_2$.

Figure 9: Powder X- ray diffraction of intercalated Bentonite with 90 % $FeCl_3$ + 10 % $FeCl_2$

Note: M: Montmorillonite, C: Cristobalite, Q: Quartz, H: Hematite (Fe_2O_3), Mt: Magnetite (Fe_3O_4).

3.3. FT-IR Characterization of Montmorillonite clay samples.

Figures (10-16) shows the FT -IR patterns of crude, activated initiated Montmorillonite clay mineral and those of iron (Fe II, Fe III) montmorillonite nanocomposites. Crude clay FT-IR pattern (Figure 10) showed absorption band at 3960 cm^{-1} & 3880 cm^{-1} corresponding to free – OH starching vibrations , 3620 cm^{-1}(Al-Al-OH) (Si-OH-Al) corresponding to starching vibration of structural OH groups coordinating to Al-Al pair or Si-OH-Al. Adsorbed water gives a broad bands from 3547 cm^{-1} to 3394 cm^{-1} corresponding to H2O stretching vibration . (Al & Si) bound water molecules gives H-O-H stretching vibration bond at 1647cm^{-1}. Also thee bands at 1531 cm^{-1}, 1423 cm^{-1} and 1365 cm^{-1} corresponding to H...O...H weak stretching vibration. Out-of-plain Si-O stretching vibration appear at 1153 cm^{-1}. The complex tow broad band around 1010 cm^{-1}, 947 cm^{-1} belongs to In-

plain layered silicates (Si-O) stretching vibration. Bands at 912 cm^{-1} belongs to Al-Fe- OH bending vibration and 839 cm^{-1} belongs to Al-Mg-OH bending vibration. Also bands at 796 cm^{-1} belong to Silicate, Mg-Fe-OH bending vibration, at 767 cm-1 belongs to Si-O-Si bending vibration, at 611 cm^{-1} belongs to Ca-O stretching vibration, at 538 cm^{-1} belongs to Al-O stretching vibration, and a tow bands at 567 cm^{-1} & 468 cm^{-1} refer to Si-O bending vibration. Finally the bands at 432 cm^{-1} related to Al-O-Si, Si-O-Si bending vibration. FT- IR spectrum of initiated bentonite (Figure 11) showed the same bands of (Figure 10) but with higher transmittance percent and sharper than bands of FT- IR spectrum of natural bentonite. The activated initiation process of bentonite clay mineral to H- form Montmorillonite clay mineral using ion – exchange technique lead to the removal of all ions present between the clay layers by the active protons displacement and this explains the disappearance of band at 567 cm^{-1} which belongs to (Hematite) Fe_2O_3 stretching vibration and band at 611 cm^{-1} belongs to Ca-O stretching vibration. comparing the FT-IR patterns (Figures 12 - 16) with that of initiated bentonite (Figure 11) We noticed the appearance of a new peaks (Figure 12) at 480 cm^{-1} which belongs to (Hematite) Fe_2O_3 stretching vibration, at 594 cm^{-1} belongs to (Magnetite Fe_3O_4) stretching vibration, and at 667 cm^{-1} belongs to Fe-O stretching vibration. (Figure 13) show also a peak at 667 cm^{-1} belongs to Fe-O stretching vibration. (Figure 14) show also a peak at 586 cm^{-1} belongs to (Magnetite Fe_3O_4) stretching vibration. (Figure 15) show also a peak at 675 cm^{-1} belongs to Fe-O stretching vibration. Finally (Figure 16) show also a peak at 586 cm^{-1} belongs to (Magnetite Fe_3O_4) stretching vibration and at (555 cm^{-1} & 489 cm^{-1}) belongs to (Hematite) Fe_2O_3 stretching vibration [26].
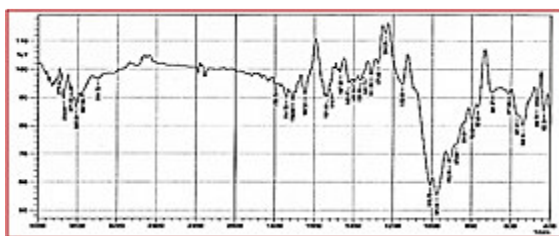

Figure 10: FT- IR spectrum of Crude Bentonite.
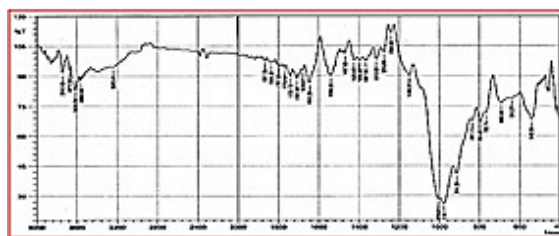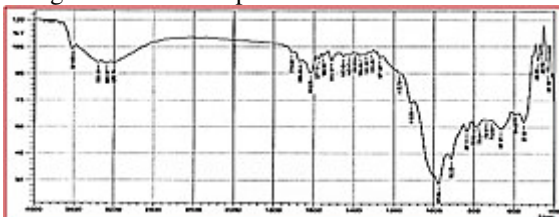

Figure 11: FT-IR of initiated Bentonite.

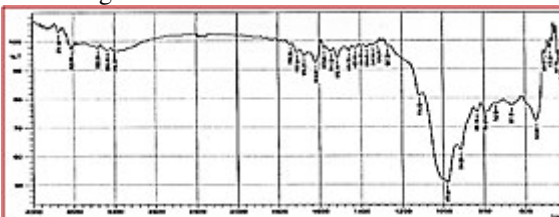Figure12: FT-IR of Bentonite intercalated with 100 % $FeCl_2$ saturated solution.

Figure 13: FT-IR of Bentonite intercalated with 100% $FeCl_3$ saturated solution.
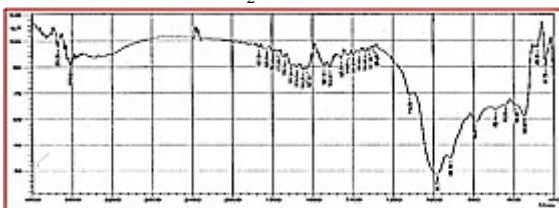

Figure 14: FT-IR of Bentonite intercalated with 50 % $FeCl_3$ + 50 % $FeCl_2$ saturated solutions.
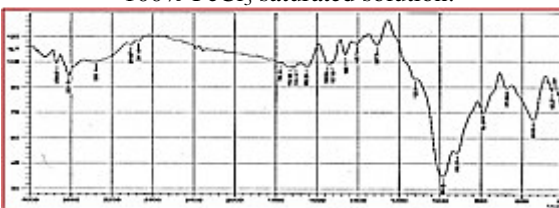

Figure 15: FT-IR of Bentonite intercalated with 40 % $FeCl_3$ + 60 % $FeCl_2$ saturated solutions.

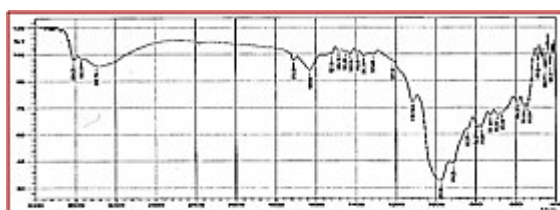Figure 16: FT-IR of Bentonite intercalated with 90 % $FeCl_3$ + 10 % $FeCl_2$ saturated solutions.

3.4. Scanning Electron Microscopy (SEM) Characterization of Montmorillonite clay samples.
Low and high magnification SEM images Figure 17 (A, B, C & D) of initiated H - form montmorillonite show a normal characteristic of layered shape Montmorillonite Clay, while in Figure 17 (E, F, G & H) of intercalated

montmorillonite with 100 % $FeCl_2$, and (I, J, K, & L) of intercalated montmorillonite with 40 % $FeCl_3$ + 60 % $FeCl_2$ showed a change in the nature of the Montmorillonite clay surface due to high intercalation of iron (Fe II, Fe III) on the external surface of clay mineral and in the interlayer space of montmorillonite. This was shown clearly in high magnification SEM images Figure 17 (D, H, & L) by having a new texture to the clay surface. Through an accurate vision of Figure 17 (H, & L) of iron (Fe II, Fe III) intercalated montmorillonite nanocomposite the needle – shaped structures were seen on the external surface of clay mineral in a complete needle like morphology composed with sharp tipped magnetic octahedron rods. (Figure 18) explain the Internal crystal structure with Directions of the body diagonal ([111] direction) and orthogonal to the cubic faces ([001] direction) are shown as arrows. These images indicate the success of the process of intercalation.
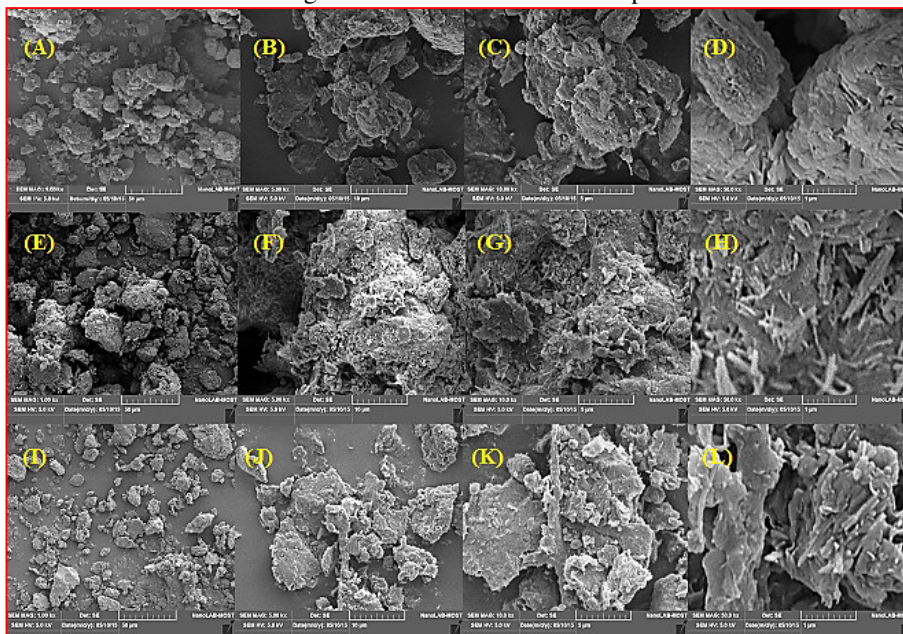

Figure 17: Low and high magnification SEM images (A, B, C, & D) of initiated H - form montmorillonite, (E, F, G & H) of intercalated montmorillonite with 100 % $FeCl_2$ solution, and (I, J, K, & L) of intercalated montmorillonite with 40 % $FeCl_3$ + 60 % $FeCl_2$ solution.
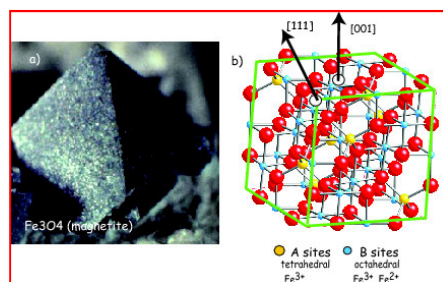

Figure 18: a) A magnetite octahedron. [Photo of Lou Perloff in the Photo-Atlas of Minerals.] b) Internal crystal structure. Directions of the body diagonal ([111] direction) and orthogonal to the cubic faces ([001] direction) are shown as arrows. Big red dots are the oxygen anions. The blue dots are iron cations in octahedral coordination and the yellow dots are in tetrahedral coordination. Fe3+ sits on the A sites and Fe2+ and Fe3+ sit on the B sites.

4. Conclusions

A new and simple method of preparation of iron (Fe II, Fe III) –montmorillonite magnetic clay hybrids was applied, depending on ion exchange technique. The intercalated bentonite samples show high Magnetic susceptibilities, Powder X- ray diffraction spectra confirmed the formation of iron oxides (Hematite Fe_2O_3), at (2θ = 24 ◦, 33◦, 34◦, 35◦, 39◦, 41◦, and 49◦), and (Magnetite Fe_3O_4), at (2θ = 36 ◦, 39◦, 42◦, and 43◦). FT-IR patterns noticed the appearance of new peaks belongs to (Hematite) Fe_2O_3 stretching vibration, Fe-O stretching vibration, and (Magnetite Fe_3O_4) stretching vibration. SEM images showed a change in the nature of the Montmorillonite clay surface. All this proves the success of (Fe II, Fe III) intercalation method in montmorillonite clay mineral and reinforce the formation of magnetic clay.

References
[1] Katayoon Kalantari,Mansor B. Ahmad, Kamyar Shameli, Mohd Zobir Bin Hussein, Roshanak Khandanlou, and Hajar Khanehzaei, Size-Controlled Synthesis of Fe_3O_4 Magnetic Nanoparticles in the Layers of Montmorillonite, Journal of Nanomaterials, Article ID 739485, 9 pages Volume 2014.

[2] Booker, N.A., Keir, D., Priestley, A., Rithchie, C.D., Sudarmana, D.L., Woods, M.A., Sewage clarification with magnetite particles. Water Sci. Technol. 123, pp. 1703– 1712, 1991.

[3] G. Li, Z. Zhao, J. Liu, and G. Jiang, "Effective heavy metal removal from aqueous systems by thiol functionalized magnetic mesoporous silica," Journal of Hazardous Materials, vol. 192, no. 1, pp. 277–283, 2011.

[4] I. Larraza, M. L´opez-G´onzalez, T. Corrales, and G. Marcelo, "Hybrid materials: magnetite-poly ethylenimine montmorillonite, as magnetic adsorbents for Cr (VI) water treatment," Journal of Colloid and Interface Science, vol. 385, no. 1, pp. 24–33, 2012.

[5] B. C. Munoz, G.W. Adams, V. T. Ngo, and J. R. Kitchin,"Stable magnetorheological fluids," Google Patents, 2001.

[6] G. Mihoc, R. Ianos¸, C. Pˇacurariu, and I. Lazˇau, "Combustion synthesis of some iron oxides used as adsorbents for phenol and p-chloro phenol removal from wastewater," Journal of Thermal Analysis and Calorimetry, vol. 112, no. 1, pp. 391–397, 2013.

[7] M. Abbas, B. Parvatheeswara Rao, S. M. Naga, M. Takahashi, and C. Kim, "Synthesis of high magnetization hydrophilic magnetite (Fe_3O_4) nanoparticles in single reaction—surfactant less polyol process," Ceramics International, vol. 39, no. 7, pp. 7605– 7611, 2013.

[8] Tam´as Szab´o, Aristides Bakandritsos, Vassilios Tzitzios, Szilvia Papp, L´aszl´o K˝or¨osi, G´abor Galb´acs, KuanyshbekMusabekov, Didara Bolatova, Dimitris Petridis and Imre D´ek´, Magnetic iron oxide/clay composites: effect of the layer silicate support on the microstructure and phase formation of magnetic nanoparticles, IOP Publishing, Nanotechnology, 18, 285602, (9 pp), 2007.

[9] Booker N A, Keir D, Priestley A, Rithchie C D, Sudarmana D L and Woods M A Water Sci. Technol. 123, p.1703, 1991.

[10] Oliveira L C A, Rios R V R A, Fabris J D, Sapag K, Garg V K and Lago R M Appl. Clay Sci. 22, p.169, 2003.

[11] Stavroyiannis S, Panagiotopoulos I, Niarchos D, Christodoulides J A, Zhang Y and Hadjipanayis G C Appl. Phys. Lett. 73, p. 3453, 1998.

[12] Tsang S C, Yu C H and Tam K. J. Phys. Chem. B 110 16914, 2006.

[13] Lee I S, Lee N, Park J, Kim B H, Yi Y-W, Kim T, Kim T K, Lee I H, Paik S R and Hyeon T J. Am. Chem. Soc. 128, 10658, 2006.

[14] Mornet S, Vasseur S, Grasset F and Duguet E J. Mater. Chem. 14, 2161, 2004.

[15] Sathe T R, Agrawal A and Nie S Anal. Chem. 78, 5627, 2006.

[16] Wang D, He J, Rosenzweig N and Rosenzweig Z 2004 Nano Lett. 4 409 magnetic nanoparticles, IOP Publishing, Nanotechnology 18, 285602 (9pp), 2007.

[17] Mazeyar Parvinzadeh • Shima Eslami, Optical and electromagnetic characteristics of clay–iron Oxide nanocomposites, Chem Intermed 37: pp.771–784, Springer Science 2011.

[18] Cadena, F., Rizvi, R., Peter, R.W., Feasibility studies for the removal of heavy metal from solution using tailored bentonite, hazardous and industrial wastes. Proceedings 22nd Midi Atlantic Industrial Waste Conference, Drexel University. 77 pp. 1990.

[19] Bailey, S.E., Olin, T.J., Bricka, R.M., Adrian, D.D., A review of potentially low cost sorbents for heavy metals. Water Res. 33, 2469, 1999.

[20] A. K. Mishra, S. Allauddin, R. Narayan, T. M. Aminabhavi, and K. V. S. N. Raju, "Characterization of surface-modified montmorillonite Nano composites," Ceramics International, vol. 38, no. 2, pp. 929–934, 2012.

[21] M. Fan, P. Yuan, J. Zhu et al., "Core-shell structured iron nanoparticles well dispersed on montmorillonite," Journal of Magnetism and Magnetic Materials, vol. 321, no. 20, pp. 3515– 3519, 2009.

[22] A Espinosa, A Serrano, A Llavona, J Jimenez de la Morena, M Abuin, A Figuerola, T Pellegrino, J F Fernandez, M Garcia-Hernandez, G R Castro, and M A Garcia, On the discrimination between magnetite and Maghemite by XANES measurements in fluorescence mode, Measurement Science and Technology, 23, 015602 (6pp) 2012 .

[23] Mohammed H. Abdul Latif *, Mohammed A.K. Alsouz, Ibtisam J. Dawood, Amer J. Jarad, Analytical Profile of 4 - (4-Nitro Benzene Azo) - 3 - Amino Benzoic Acid on a Surface of Natural Granulated Calcined Iraqi Montmorillonite Clay Mineral, via Columnar Method, Journal of Chemical and Process Engineering

Research, Vol.19, pp. 1-14, 2014.

[24] M. Onal; "Changes in crystal structure, thermal behavior and surface area of bentonite by acid activation"; Commun. Fac.Sei. llniv. Ank. Series B,V. 53(1) , pp.. 1-14 2007.

[25] Tam´as Szab´o, Aristides Bakandritsos, Vassilios Tzitzios, Szilvia Papp, L´aszl´o K˝or¨osi, G´abor Galb´acs, KuanyshbekMusabekov5, Didara Bolatova5, Dimitris Petridis2 and Imre D´ek´any , Magnetic iron oxide/clay composites: effect of the layer silicate support on the microstructure and phase formation of magnetic nanoparticles, Nanotechnology 18, pp.9, IOP Publishing, 2007.

[26] Mazeyar Parvinzadeh • Shima Eslami, Optical and electromagnetic characteristics of clay–iron oxide nanocomposites, Chem Intermed, 37: pp.771–784 Springer Science, 2011.

The IISTE is a pioneer in the Open-Access hosting service and academic event management. The aim of the firm is Accelerating Global Knowledge Sharing.

More information about the firm can be found on the homepage:
http://www.iiste.org

CALL FOR JOURNAL PAPERS

There are more than 30 peer-reviewed academic journals hosted under the hosting platform.

Prospective authors of journals can find the submission instruction on the following page: http://www.iiste.org/journals/   All the journals articles are available online to the readers all over the world without financial, legal, or technical barriers other than those inseparable from gaining access to the internet itself. Paper version of the journals is also available upon request of readers and authors.

MORE RESOURCES

Book publication information: http://www.iiste.org/book/

Academic conference: http://www.iiste.org/conference/upcoming-conferences-call-for-paper/

IISTE Knowledge Sharing Partners

EBSCO, Index Copernicus, Ulrich's Periodicals Directory, JournalTOCS, PKP Open Archives Harvester, Bielefeld Academic Search Engine, Elektronische Zeitschriftenbibliothek EZB, Open J-Gate, OCLC WorldCat, Universe Digtial Library , NewJour, Google Scholar